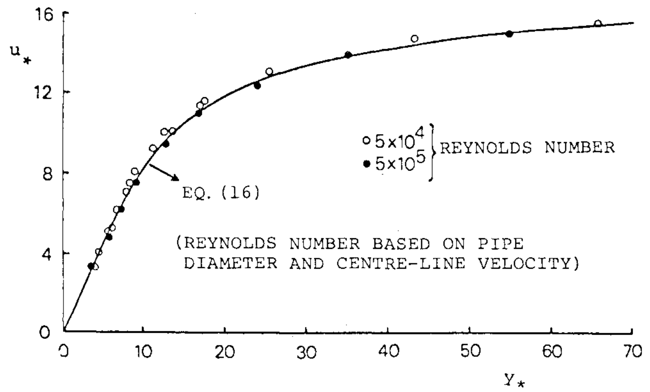

Fig. 1 Comparison of formula with pipe-flow data of Laufer in viscous sublayer and buffer zone.

the Stanford Conference. After integrating Eq. (9) and combining with Eqs. (13) and (14), a good deal of algebra yields the following closed-form expression for the velocity distribution over a smooth wall which is valid continuously from the wall up to the freestream:

$$u_* = 5.424\tan^{-1}\left[\frac{2y_* - 8.15}{16.7}\right] + \log_{10}\left[\frac{(y_* + 10.6)^{9.6}}{(y_*^2 - 8.15y_* + 86)^2}\right] - 3.52 + 2.44 \times \left\{\Pi\left[6\left(\frac{y}{\delta}\right)^2 - 4\left(\frac{y}{\delta}\right)^3\right] + \left[\left(\frac{y}{\delta}\right)^2\left(1 - \frac{y}{\delta}\right)\right]\right\} \tag{16}$$

where $u_* = u/u_0$ and $y_* = yu_0/\nu$.

Discussion

As far as the author is aware, there is no other explicit expression available for the smooth-wall velocity distribution which satisfies both the momentum and continuity equations near the wall while satisfying the four boundary conditions: $y=0$, $u=0$ and $\mathrm{d}u_*/\mathrm{d}y_* = 1$; $y=\delta$, $u=U_\infty$ and $\mathrm{d}u/\mathrm{d}y = 0$. (For $y=\delta$, $y_* \to \infty$ is regarded as a limiting boundary condition.)

The description of the mean velocity distribution afforded by Eq. (16) is in excellent agreement with Laufer's[5] experimental data near the wall, as is shown in Fig. 1. Away from the wall, as $y \to \infty$, Eq. (16) approaches Eq. (15) asymptotically and so the logarithmic and outer regions are adequately described (see Ref. 7).

Conclusions

It has been shown how the cubic law for the variation in eddy kinematic viscosity very near the wall can be combined with the linear law in the logarithmic region by the use of a simple interpolation formula. This formula leads to an explicit closed-form expression for the velocity distribution over a smooth wall in a turbulent boundary layer which should prove useful in studies of heat and mass transfer and turbulent boundary-layer procedures.

Acknowledgments

The author would like to thank J. H. Preston for many useful comments and the U.K. Science Research Council for financial sponsorship.

References

[1] Dean, R. B., "A Single Formula for the Complete Velocity Profile in a Turbulent Boundary," *Journal of Fluids Engineering*, Vol. 98, Dec. 1976, pp. 723-726.

[2] Spalding, D. B., "A Single Formula for the Law of the Wall," *Journal of Applied Mechanics, Transaction of the ASME*, Series E., Vol. 83, 1961, p. 455.

[3] Finley, P. J., Phoe, K. C., and Poh, C. J., "Velocity Measurements in a Thin Turbulent Water Layer," *La Houille Blanche*, Vol. 21, 1966, p. 713.

[4] Reichardt, H., "Volständige Darstellung der turbulenten Geschwindigkeitsverteilung in glatten Leitungen," *Zeitschrift für Angewandte Mathematik und Mechanik*, Vol. 31, 1951, p. 208.

[5] Laufer, J., "The Structure of Turbulence in Fully-Developed Pipe Flow," NACA Report 1174, 1954 (formerly TN 2954).

[6] Coles, D. E., "The Law of the Wake in the Turbulent Boundary Layer," *Journal of Fluid Mechanics*, Vol. 1, Pt. 2, 1956, p. 191.

[7] Coles, D. E., "Computation of Turbulent Boundary Layers," 1968 AFOSR-IFP-Stanford University Conference Proceedings, Vol. 2, Stanford Univ., 1968.

[8] Hinze, J. O., *Turbulence*, McGraw-Hill, New York, 1959.

[9] Moses, H. L., "The Behavior of Turbulent Boundary Layers in Adverse Pressure Gradients," Rept. 73, Gas Turbine Lab., Massachusetts Inst. of Tech., 1964.

[10] Cornish, J. J. III, "A Universal Description of Turbulent Boundary Layer Profiles With or Without Transpiration," Research Rept. 29, Mississippi State Univ., Aero Physics Dept., 1960.

[11] Bull, M. K., "Velocity Profiles of Turbulent Boundary Layers," *The Aeronautical Journal*, Vol. 73, 1969, p. 143.

[12] Granville, P. S., "A Modified Law of the Wake for Turbulent Shear Flows," Rept. 4639, U. S. Naval Ship Research and Development Center, 1975.

Some Measurements in Radial Free Jets

Rajni P. Patel*

University of Nairobi, Nairobi, Kenya

Introduction

IN many fluid flow problems of practical importance, one encounters free shear flows such as jets, wakes, and mixing layers. In the class of jet flows there is a flow configuration known as a radial jet which has not yet received much attention. Recently Witze and Dwyer[1] have investigated the turbulent radial jets. In their investigation the radial jets have been classified as "constrained radial jets" and "impinged radial jets." In this investigation a distinct new category of radial jets has been introduced to distinguish it from the other two categories. This is the ideal radial free jet. Essentially it is similar to the impinged jet, but it has small separation distance between the nozzles to avoid the initial developing regions of the axisymmetric jets. The constrained radial jet has been investigated by Heskestad,[2] and some measurements on the ideal radial free jet have been reported by Patel et al.[3]

From these investigations it is noted that the measurements of the impinged radial jets reported so far are limited. For example, Witze and Dwyer selected nozzle spacings greater than 20 times the nozzle diameter, thus limiting the field of investigation to $(r/s) < 0.5$. With such large separation distances the impinged radial jets produced by them were in fact a result of the two interacting axisymmetric turbulent jets that had already undergone some development.

The radial jet investigated by Patel et al.[3] had the constraint ratio of 3.16, and the corresponding separation distance s was $0.316D$. However, their measurements were confined within the region $(r/s) \leq 20$. This limitation was imposed because the fan pressure supplying air to the nozzles was not sufficient to obtain meaningful results beyond

Received Nov. 14, 1977; revision received Jan. 16, 1979.

Index category: Jets, Wakes, and Viscid-Inviscid Flow Interactions.

*Dean, Faculty of Engineering. Member AIAA.

$(r/s)>20$. In spite of the large constraint ratio compared with those of the impinged jets of Witze and Dwyer, the results of Patel et al. indicated that it is possible to produce a self-preserving radial free jet.

The purpose of this investigation was to extend the range of measurements and at the same time investigate the influence of nozzle lengths on the radial free jets. It was, therefore, necessary to use the same (s/D) ratio and vary the length of the nozzles. For this reason present measurements were obtained in a completely different experimental apparatus, and they are compared with the results of Patel et al.

Experimental Apparatus

To investigate the radial free jets with small spacing between the nozzles, two experimental setups were designed. In the first apparatus the nozzle were made from a precision seamless tubing having a length-to-diameter ratio of about 62.7. The internal diameter of the nozzle was 10.04 mm, and the ratio of nozzle diameter to spacing between nozzles was 3.16. The air from a radial fan was supplied to a settling chamber approximately 1 m^3 in size. The nozzles were connected to the settling chamber outlet by identical pipe branches. The complete details for this apparatus are given in Ref. 3.

In the second apparatus high-pressure air was used. The nozzles were made of similar seamless tubing as above but having a length-to-diameter ratio of about 14.92. This apparatus consisted of two identical plenum chambers having the dimensions of 20.3 cm on each side and made from 3.175 mm-thick mild steel plate. The nozzle was fixed at the center of a face on each chamber, and the air supply was provided from the opposite face. Each plenum chamber was provided with a static pressure tap so that the pressure within the chamber could be monitored. The chambers were mounted on two horizontal tables in such a way that the nozzle outlets faced each other to produce the radial free jet. The other details of this apparatus are given by Halfan and Mureithi.[4]

All measurements reported here were made with a pitot tube of 0.0762 cm outside diameter with chamfered lip. The flowfield was investigated for symmetry, and it was found that the radial jets had satisfactory axial symmetry.

Nondimensional Mean Velocity Profiles

Figure 1 shows the typical nondimensional mean velocity profiles measured in the radial free jets. For comparison the results of Witze and Dwyer[1] are included in this figure. Furthermore, the two commonly used mathematical functions to represent nondimensional mean velocity profiles in free turbulent shear flows are also shown in this figure.

Comparison of the present results with those of Witze and Dwyer indicates that the present results for $z/z_{m/2}\leq 1.0$ are in agreement with their results, but beyond $z/z_{m/2}>1$ their results deviate from the present results. They have attributed this behavior to the high entrainment rate. Indeed one would expect the high entrainment rate in their investigation of the impinged radial jet in view of the influence of the initial development of the axisymmetric jets.

Of the two mathematical functions, namely $U/U_0=\text{sech}^2(0.881z/z_{m/2})$ and $U/U_0=e^{-0.693(z/z_{m/2})^2}$, the latter fits the present results very well. It should be noted that the exponential function has been a better representation of the nondimensional mean velocity profiles for other free shear flows as well.

Growth of Radial Free Jets

The theoretical analysis indicates that the turbulent radial free jets should grow linearly and that the hypothetical origin should be situated on the z axis. To confirm this, Fig. 2 is presented, in which the jet width is represented by $z_{m/2}$. Note that $z_{m/2}$ is the value of z where $U=\frac{1}{2}U_0$. In this figure the results of Witze and Dwyer[1] and Patel et al.[3] are also included.

From the figure it can be seen that the turbulent radial free jets grow linearly and the hypothetical origin is located on the z axis. The results of Patel et al. are in agreement with the present results. Note that the deviation of the results of Witze and Dwyer is due to different jet configurations. As mentioned before, the impinged radial jet of Witze and Dwyer appears to have been affected by the initial developments of the axisymmetric jets. The presence of the initial developing regions, in which there is strong entrainment of the surrounding fluid, make the radial jet grow at a faster rate. These measurements suggest that for the radial free jets having small nozzle separation distances $(s/D\leq 0.31)$, the rate of growth is 0.115 and for those having $20<s/D<42$, the rate of growth is 0.37.

Variation of Centerline Velocities

Figure 3 shows the variation of the centerline velocities in the radial free jets. The jet exit velocity U_j is measured at $r=D/2$. From the figure it can be seen that the centerline velocity varies inversely with the radial distance, and the measurements of Patel et al. are in agreement with the present results. However, it should be pointed out that measurements below $r/s\simeq 18$ deviate from the straight line, $U_j/U_0=1.45(r/s-10)$. Within the range $2.5\leq(r/s)\leq 18$ the variation of the centerline velocity may be represented by $U_j/U_0=0.8(r/s-2.5)$. For interest one set of results of Fig. 13 of Ref. 1 is replotted using enlarged scales, and this is included as an inset in Fig. 3. It can be seen that the variation of the centerline velocity in their investigation is nonlinear, and the rate of centerline velocity decay is substantially greater than that observed in the present investigation. This was expected since the rate of growth for their impinged radial jets was quite

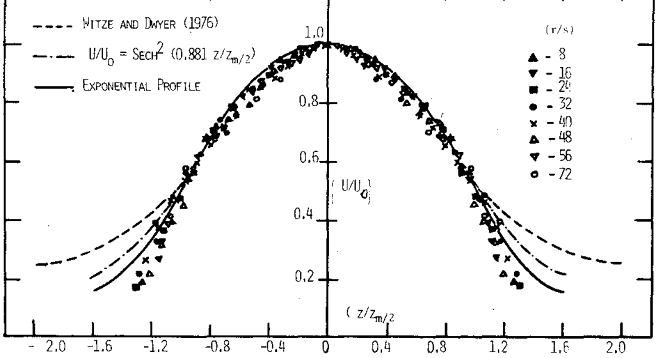

Fig. 1 Nondimensional mean velocity profiles.

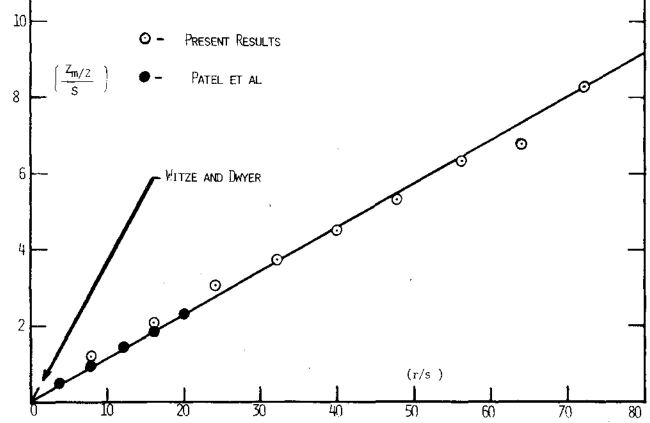

Fig. 2 Growth of radial free jets.

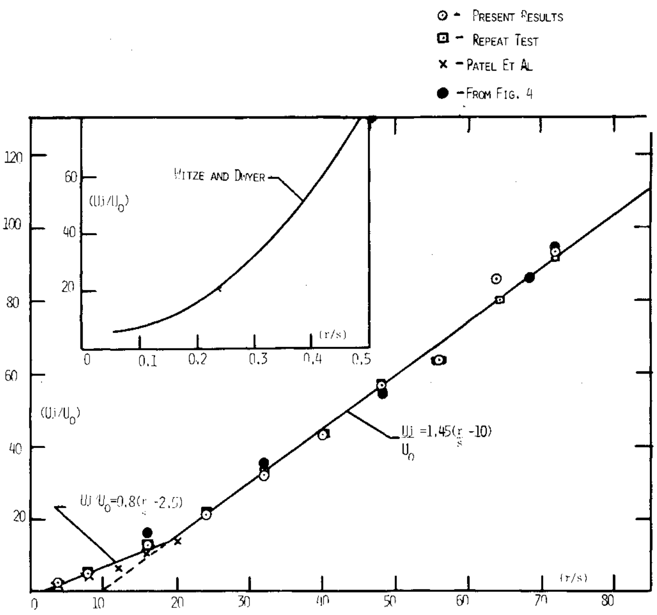

Fig. 3 Variation of centerline velocities.

high. Physically the flowfield for their impinged radial jet would be similar to the one produced by a radial free jet between two vortex rings, and boundary layer approximations will not be applicable in such a flowfield.

Conclusions

The experimental results of a turbulent radial free jet reported here show that it is possible to produce an ideal radial free jet. A necessary condition for the production of the ideal radial free jet is that the spacing between the two identical and opposing impinging jets should be quite small.

The measurements presented in this paper cover a large range of (r/s) compared to the previous investigations. From the measurements it is concluded that nondimensional mean velocity profiles within the range $4 \le r/s \le 72$ can be represented by an exponential function, $U/U_0 = \exp[-0.693(z/zm/2)^2]$. Furthermore, the radial jet grows linearly, with the rate of growth equal to 0.1155, and the hypothetical origin is situated on the z-axis. Also the centerline velocity varies inversely with the radial distance, i.e., $U_0 \propto 1/r$. It appears that below $r/s \simeq 18$ the variation of the centerline velocity is given by $U_j/U_0 = 0.8(r/s - 2.5)$ and above $(r/s) = 18$ it is given by $U_j/U_0 = 1.45\ (r/s - 10)$. Clearly around $(r/s) = 18$ the rate of decay of the centerline velocity changes, and this may be due to the presence of the core region and the initial boundary layers in the nozzles. The length of the nozzles appears not to have affected the measurements.

Acknowledgment

The author wishes to thank H. Halfan and A. K. Mureithi for conducting the experiments.

References

[1]Witze, P. O. and Dwyer, H. A., "The Turbulent Radial Jet," *Journal of Fluid Mechanics*, Vol. 75, Pt. 3, 1976, pp. 401-417.

[2]Heskestad, G., "Hot-Wire Measurements in a Radial Turbulent Jet," *Journal of Applied Mechanics*, Vol. 88, 1966, pp. 417-424.,

[3]Patel, R. P., Olupot L'ingorot, P. H., and Wekeika, G. B., "Gross Features of a Turbulent Radial Jet," *The Journal of Engineering Education and Research in Tropical Africa*, Vol. 4, No. 1, 1978, pp. 26-34.

[4]Halfan, H. and Mureithi, A. K., "An Investigation of Radial Free Jet," Project Rept. No. 15, University of Nairobi, Kenya, Mechanical Engineering Dept., 1977.

Hysteresis Zone or Locus—Aerodynamic of Bulbous Based Bodies at Low Speeds

Eugene E. Covert*
Massachusetts Institute of Technology, Cambridge, Mass.

IN Ref. 1, Ericsson and Reding discuss problems associated with measuring the one-degree-of-freedom damping in pitch $(C_{m_q} + C_{m_{\dot\alpha}})$ on slender axially symmetric bodies. In particular, they cite problems of hysteresis in data obtained from tests of cones with hemispherical bases shown in Figs. 5 and 6 of Ref. 1. This hystersis is a generalization of their earlier work,[2] where it is argued that interaction between the rear wake and a bulbous base causes the damping in pitch derivative to change sign and hence to have a destabilizing tendency. In these references, the idea of a hysteresis loop is introduced. The point of the presentation in Ref. 1 is to help the analyst to decide whether or not the aberration in the data is real or is facility induced. We are adding some data here which, unfortunately, compound the dilemma rather than clarifying it. The dilemma is compounded because the data suggest that a well-defined hysteresis locus does not seem to exist. Rather, if the experiment is repeated several times, the entire hysteresis region seems to fill with data rather than trace out a specific hysteresis locus. Consequently, one rather suspects that the phenomenon is governed by the whim of the fluid to separate. In this respect, the problem is rather like that reported by Lamont and Hunt.[3] Additional data show that a roughened body or a dummy sting causes a support interference that tends to reduce the hysteresis zone to a smaller, sometimes negligible region.

Figures 1 and 2 show normal force coefficient and pitching moment coefficient for a magnetically suspended bulbous base cone when a sting is near the base. The sting is either aligned with the cone axis or is 1 or 2 deg below it. The data are generally well behaved although they suggest that the linear region is relatively ill defined. Also shown on these figures is a zone where the data are not unique. This lack of uniqueness is attributed to unsteady separation from the bulbous base. Note, however, this is relatively small, extending over ½ deg or less.

Reference 4 presents data on the aerodynamic characteristics of several magnetically suspended bulbous or partially bulbous based cones. Figures 3 and 4 show that the presence of a sting caused a well-defined lift and moment coefficient curve, while in the absence of a sting a small hysteresis zone exists. The hysteresis zone is hatched in. No data were presented at the zero angle of attack point because the model motion was considered excessive. Figure 5 shows the lift coefficient again with and without a tripped boundary layer, and with no sting. The hatched hysteresis zone corresponds to that given in Fig. 3. The hysteresis zone for laminar flow is outlined by the dash-dot line. The arrows show the direction of the sequence of points, up or down. The lack of symmetry is believed due to an insufficient amount of data. Figures 6 and 7 show the same sort of effect on pitching moment and drag coefficient, although the hysteresis zones are more symmetric.

Received May 24, 1978; revision received Dec. 21, 1978.

Index categories: Jets, Wakes, and Viscid-Inviscid Flow Interactions; Aerodynamics; LV/M Dynamics and Control.

*Professor of Aeronautics and Astronautics. Fellow AIAA.